ELSEVIER

Catalysis Today 56 (2000) 403–414

CATALYSIS TODAY

www.elsevier.com/locate/cattod

XPS and SIMS characterization

V.I. Bukhtiyarov (RU-1) *

Boreskov Institute of Catalysis, Prospekt Akademika Lavrentieva 5, 630090 Novosibirsk, Russia

Contributors: P. Albers (D-2), M. Baerns (D-1), B.S. Bal'zhinimaev (RU-1), G.C. Bond (GB-1), A. Brueckner (D-1), V.I. Bukhtiyarov (RU-1), M. Delamar (F-7), P. Delichere (F-1), P. Druska (D-1), L. Gengembre (F-6), M.J. Genet (B-2), M. Guelton (F-6), J. Kiwi (CH-2), J.Ph. Nogier (F-2), I.P. Prosvirin (RU-1), A.O. Taylor, I. York (GB-1)

Abstract

XPS study V_2O_5–WO_3/TiO_2 mixed oxide catalysts for Selective Catalytic Reduction (SCR) of NO_x carried out by researchers from ten different laboratories shows good reproducibility of the chemical shift results. The binding energies of the corresponding core level spectra allow us to identify the chemical states of main elements as Ti(IV), V(V) and W(VI). No other oxidation states for these elements were observed both for fresh/used and for crushed/monolith samples. Discrepancy in quantitative data can be proposed to arise from the heterogeneity of their composition as a function of depth. This suggestion is confirmed by SIMS data and ion etching experiments which indicate surface location of V_2O_5 phase, as well as impurity ones, with respect to TiO_2 and WO_3 and their redistribution as result of catalyst operation.

Keywords: Oxide catalysts; Characterization; XPS; SIMS

1. Introduction

Over the last two decades X-ray photoelectron spectroscopy (XPS) has become a routine method for studying and characterization of a solid. There are two reasons which have led to the extension of the methods developed in the 1960s by Siegbahn [1]. One of them is the fact that except for hydrogen all chemical elements exhibit photoelectron spectra, XPS being sensitive not only to elemental composition, but also to the chemical state of the element studied. This is responsible for the other name for XPS which is well-known for chemists — electron spectroscopy for chemical analysis (ESCA). The other reason for the wide application of XPS is appearance of a number of companies that have produced and are producing XPS spectrometers commercially: Vacuum Generators (UK), Leybold-Heraus (Germany), Riber (France), Scienta (Sweden), etc. However, various approaches to construction of the electron spectrometers, different geometry of the electron energy analyzer, etc. make it difficult to compare the results obtained by different researchers using different spectrometers even for identical systems. To tackle this problem we have carried out an XPS study of EUROCAT mixed oxide catalysts carried out by different research groups using the same samples. We show that chemical states of the observed elements are identical as defined by all research groups, but there are some discrepancies in the quantitative analysis. Possible reasons for the latter problem are discussed. Additional information about distribution of the element on sample depth have been obtained using secondary ion mass spectroscopy (SIMS).

* Tel.: +7-383-2-34-3767; fax: +7-383-2-34-4770.
E-mail address: vib@catalysis.nsk.su (V.I. Bukhtiyarov (RU-1)).

0920-5861/00/$ – see front matter
PII: S0920-5861(99)00300-4

2. Experimental

2.1. Equipment

XPS spectrometers of various types produced by different companies have been used in this comparative study, amongst them are a VG ESCALAB High Pressure (RU-1), a VG ESCALAB (F-1, D-1, GB-1), an LHS 10 (F-6), a SSI M Probe (F-2 and F-7), an SSX-100/206 (B-2) and a MAX 100 (CH-2 and D-2). Both monochromated (F-2 and F-7, B-2) and non-monochromated (RU-1, F-1, F-6, CH-2 and D-2, D-1, GB-1) Al Kα or Mg Kα irradiations were used in this work. Before the experiments most of the spectrometers were calibrated against E_b(Au $4f_{7/2}$) = 84.0 (83.98) eV and E_b(Cu $2p_{3/2}$) = 932.6 eV [2]. To avoid any charging effect appearing for the oxide catalysts we used both flood guns (F-2 and F-7, B-2, CH-2 and D-2, D-1) and the method of internal standardization, the Ti $2p_{3/2}$ (RU-1, F-6, GB-1) or C 1s (F-1) lines being taken as internal references with a binding energy of 459.0 and 284.7 eV, respectively [3,4].

2.2. Samples

The V_2O_5–WO_3/TiO_2 catalysts as monoliths have been provided by "Austrian Energy and Environment" (Wien): as prepared (fresh) and used for 9000 h in SCR reaction. Some of the participants studied the samples as monoliths (F-2 and F-7, F-1), some of us as crushed powders (F-6, CH-2 and D2), and three groups both as monoliths and as powders (RU-1, B-2, GB-1). Monolith samples represent small irregular pieces of about 0.5–1 cm^2 of monolith which were cut from the whole, whereas the crushed samples were prepared by grinding the corresponding monoliths in an agar mortar. Monolith or crushed samples were mounted on the standard holders both through double-sided adhesive tape (RU-1, F-1, F-2 and F-7, B-2, GB-1) or directly: from alcohol emulsion (F-6) or pressing into gold or stainless steel meshes (B-2, CH-2 and D-2). Usually, XPS spectra were taken immediately after loading the samples without any pretreatment or heating, except where an activation procedure has been used to remove undesired impurities from the atmosphere, viz. heating under dry air at 673 K.

2.3. SIMS

To measure SIMS spectra a Leybold IQ 12/38 ion gun with Wien filter has been used (CH-2 and D-2). The filter was necessary to avoid the undefined additional sputter effect/sputter contribution by means of accelerated reneutralized particles. Argon (purity 99.999%, Messer-Griesheim) was used as working gas for SIMS experiments. Mass scan in the range of 0–220m/z was recorded using a Balzers QMG 511 quadropole mass spectrometer. Electronic gating was used to avoid crater edge or periphery effects. Charge compensation was performed using a regulated flood gun.

3. Results and discussion

3.1. Chemical characterization

Fig. 1 shows survey spectra of the fresh and used samples measured both as powders and as monoliths. One can see that lines characteristic not only of the mixed oxide elements (V, W, Ti, O), but also of some impurities (C, Si, Al, Mg) are present in the spectra. Furthermore, the participants who have studied the used catalyst as monolith have noted the appearance of lines characteristic of lead and sulfur (Fig. 1b). The grinding of this catalyst results in disappearance of these lines (Fig. 1a) indicating the presence of the elements on the external surface of monolith only. Before starting the analysis of the corresponding narrow regions, it should be noted that the complex composition of the system results in overlapping of a number of XPS peaks. A major difficulty of this type arises from the superposition of W 4f doublet (between 30–37 eV) with Ti 3p (about 37.7 eV), W $5p_{3/2}$ (about 41.8 eV) and V 3p (about 41.7 eV) [3]. Thus, this peak is unsuitable for XPS characterization of tungsten on the V_2O_5–WO_3/TiO_2 catalysts. Therefore, the W $4d_{5/2}$ peak has been selected as more reliable signature, even if it is broader. Nevertheless, possible simulation of the W 4f region has been made by some participants. A set of narrow XPS spectra of the main elements for the crushed fresh sample is shown in Fig. 2. One can see that the O 1s spectrum exhibits a complex shape and consists of at least two lines, whereas one narrow

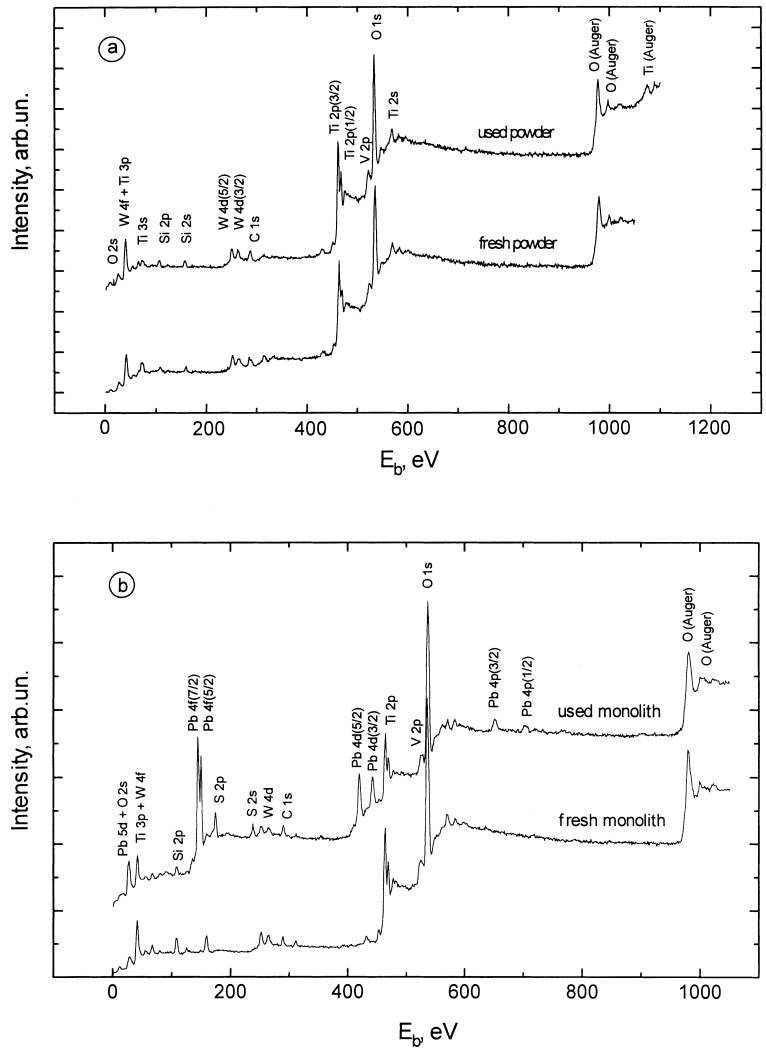

Fig. 1. Survey spectra measured for the fresh and used catalysts studied as powders (a) or as monoliths (b).

line can be used to approximate XPS spectra of the other main elements: Ti $2p_{3/2}$, V $2p_{3/2}$ and W $4d_{5/2}$.

Using such spectra, the values of core level binding energies (E_b) have been determined for all samples. These data are summarized in Tables 1 and 2 for the fresh and used catalysts, respectively. Comparison of the data demonstrates that all the binding energies are close for all powdered and monolith samples, so the mean values for the fresh and used samples can be calculated and used for analysis. Table 3 contains not only the mean values of binding energies of the corresponding XPS lines, but also standard deviations of the specific values provided by different groups (1–7) from their mean ones determined according to:

$$\Delta E_b = \frac{1}{n}\sum_i \left(E_b^i - \bar{E}_b\right).$$

One can see that the largest variations in E_b values (Tables 1–3) are observed for the spectra of impurities (Si 2p, Al 2p), or for the broadest W $4d_{5/2}$ spectrum

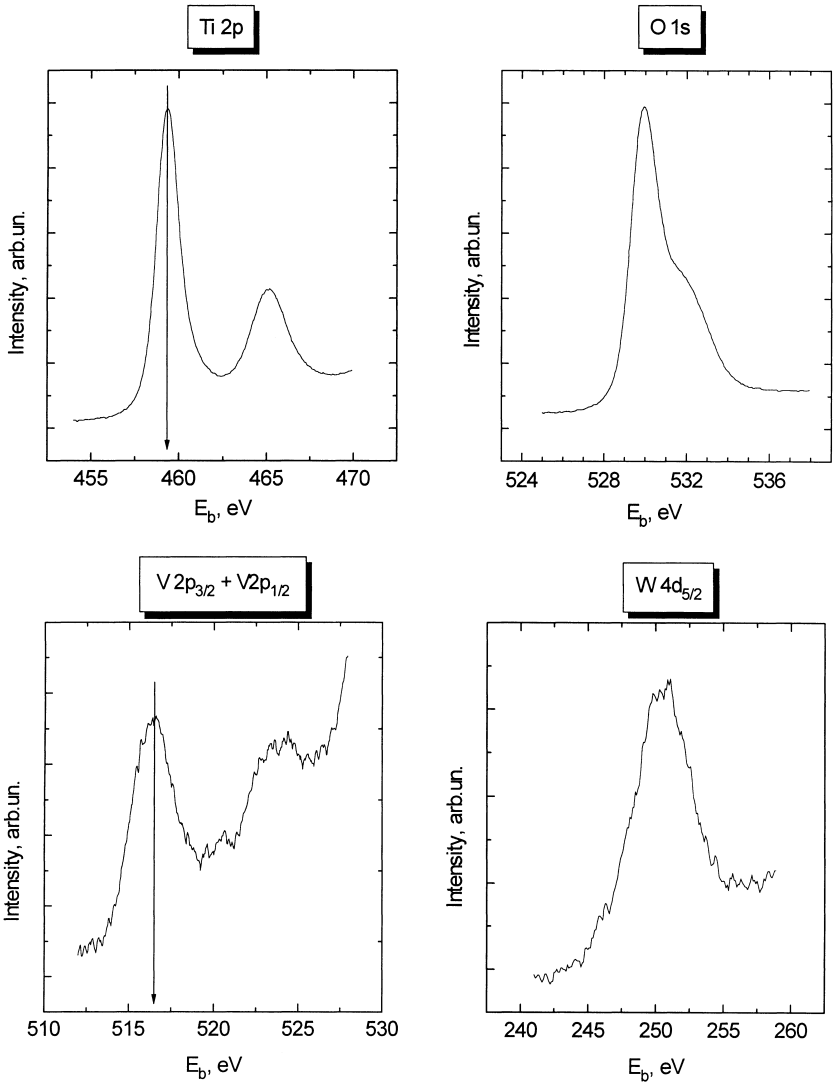

Fig. 2. Ti 2p, O 1s, V 2p and W $4d_{5/2}$ spectra for the fresh catalyst studied as powder.

(fwhm = 4.4 eV) or for the W $4f_{7/2}$ spectrum obtained by deconvolution of the overlapped region, i.e. in those cases when we could expect such difficulties objectively. The deviation in E_b observed for V $2p_{3/2}$ spectrum seems to be explained by the application of the non-monochromated X-ray irradiation utilized by a number of groups that results in overlapping of the V 2p doublet with O 1s spectrum excited by X-ray Al $K\alpha_{3,4}$ satellite. Nevertheless, one can conclude that all the binding energies measured by various research groups are close both for crushed and monolith samples. Moreover, activation of these catalysts or their operation in working conditions does not affect considerably the binding energies (Tables 1 and 2).

Assignment of most of the XPS lines is straightforward, since almost all of them can be simulated by one component with well-defined binding energies (Fig. 2). The exceptions are the O 1s and C 1s regions which consist of two or more lines. Curve fitting of the O 1s spectrum shows that it can be deconvoluted

Table 1
The core level binding energies measured for the fresh catalyst

Fresh catalyst	E_b (eV)	Comments	Reference number
Ti $2p_{3/2}$	459.0	Crushed	RU-1
	459.0	Crushed	F-6
	459.2	Crushed	B-2
	459.0	Crushed	CH-2 and D-2
	458.7	Crushed	D-1
	458.7	Crushed	GB-1
	459.0	Monolith	RU-1
	459.0	Monolith	F-2 and F-7
	459.1	Monolith	F-1
	459.0	Monolith	B-2
	458.7	Monolith	GB-1
C 1s	284.6	Crushed	RU-1
	284.7	Crushed	F-6
	284.8	Crushed	B-2
	284.5	Crushed	D-1
	284.0	Crushed	GB-1
	284.8	Monolith	RU-1
	285.2	Monolith	F-2 and F-7
	284.7	Monolith	F-1
	284.8	Monolith	B-2
	284.0	Monolith	GB-1
O ls	530.4; 533.4	Crushed	RU-1
	530.3; 533.3	Crushed	F-6
	530.5; 532.4	Crushed	B-2
	530.0; 532.5	Crushed	CH-2 and D-2
	529.9; 532.6	Crushed	D-1
	530.0; 532.4	Crushed	GB-1
	530.5; 533.2	Monolith	RU-1
	530.5; 532.9	Monolith	F-2 and F-7
	530.2; 533.0	Monolith	F-1
	530.3; 532.7	Monolith	B-2
	529.9; 532.4	Monolith	GB-1
V $2p_{3/2}$	516.9	Crushed	RU-1
	517.0	Crushed	F-6
	517.1	Crushed	B-2
	516.5	Crushed	CH-2 and D-2
	516.9	Crushed	D-1
	517.0	Crushed	GB-1
	516.9	Monolith	RU-1
	517.2	Monolith	F-2 and F-7
	516.8	Monolith	F-1
	516.6	Monolith	B-2
	517.2	Monolith	GB-1
W $4d_{5/2}$	247.7	Crushed	RU-1
	247.7	Crushed	F-6
	247.8	Crushed	B-2
	247.0	Crushed	D-1
	247.7	Monolith	RU-1
	247.8	Monolith	F-2 and F-7
	247.6	Monolith	F-1
	247.5	Monolith	B-2
	247.2	Monolith	GB-1
W $4f_{7/2}$	35.9	Crushed	B-2
	35.5	Crushed	GB-1
	36.1	Monolith	F-2 and F-7
	35.8	Monolith	B-2
Si 2p	103.8	Crushed	RU-1
	104.2	Crushed	F-6
	103.3	Crushed	B-2
	103.9	Monolith	RU-1
	103.9	Monolith	F-2 and F-7
	103.7	Monolith	F-1
	103.5	Monolith	B-2
	103.5	Monolith	GB-1
Al 2p	74.8	Crushed	F-6
	75.5	Monolith	F-1
Al 2s	120.3	Monolith	F-1

by two pronounced lines at about 530.5 and 533.0 eV, while the C 1s is best simulated by a few (up to 4) lines (B-2).

3.1.1. O 1s

The O 1s line with $E_b = 530.2 - 530.5$ eV was assigned to the lattice oxygen of the $TiO_2 + WO_3 + V_2O_5$ oxides. Such assignment is confirmed by the closeness in intensity of oxygen signals determined from the O 1s spectrum for the line with $E_b = 530.5$ eV and calculated from the normalized intensities of the metal lines using the expected stoichiometric ratios O/Me in the oxides. This ratio, $I(O_{530.5})/\sum_i I(Me_i) \cdot k_i$ (where i = Ti, W or V and k_i is the corresponding stoichiometric coefficients), has been calculated to be 1.1 ± 0.1 for all catalysts (crushed powders or monoliths, fresh or used samples). The second O 1s line ($E_b \sim 533$ eV) was assigned to SiO_2 [3,4], although it may also include some surface hydroxide.

3.1.2. Ti 2p

This line was used as reference line against $E_b = 459.0$ or 458.7 eV which is well-known to be characteristic of titanium oxide [3,4]. One group reported an asymmetry on the higher binding energy side of the Ti $2p_{3/2}$ line. This was already observed in previous investigations of V_2O_5/TiO_2 catalysts [5]. It was not possible to account for this asymmetry either using a linear background, or by supposing

Table 2
The core level binding energies measured for the used catalyst

Used catalyst	E_b (eV)	Comments	Reference number
Ti $2p_{3/2}$	459.0	Crushed	RU-1
	459.0	Crushed	F-6
	459.2	Crushed	B-2
	459.0	Crushed	CH-2 and D-2
	458.7	Crushed	D-1
	458.7	Crushed	GB-1
	459.0	Monolith	RU-1
	459.0	Monolith	F-2 and F-7
	458.8	Monolith	F-1
	458.9	Monolith	B-2
	458.7	Monolith	GB-1
C 1s	284.9	Crushed	RU-1
	284.9	Crushed	F-6
	284.8	Crushed	B-2
	284.5	Crushed	D-1
	284.0	Crushed	GB-1
	285.3	Monolith	RU-1
	285.0	Monolith	F-2 and F-7
	284.8	Monolith	F-1
	284.8	Monolith	B-2
	284.3	Monolith	GB-1
O ls	530.4; 533.2	Crushed	RU-1
	530.4; 533.2	Crushed	F-6
	530.5; 532.4	Crushed	B-2
	530.0; 532.5	Crushed	CH-2 and D-2
	530.1; 532.7	Crushed	D-1
	530.0; 532.6	Crushed	GB-1
	530.5; 533.0	Monolith	RU-1
	530.6; 533.2	Monolith	F-2 and F-7
	530.1; 532.9	Monolith	F-1
	530.2; 532.4	Monolith	B-2
	529.9; 532.4	Monolith	GB-1
V $2p_{3/2}$	516.6	Crushed	RU-1
	517.0	Crushed	F-6
	517.0	Crushed	B-2
	516.4	Crushed	CH-2 and D-2
	517.1	Crushed	D-1
	517.0	Crushed	GB-1
	516.5	Monolith	RU-1
	516.7	Monolith	F-2 and F-7
	516.6	Monolith	F-1
	516.8	Monolith	B-2
	517.1	Monolith	GB-1
W $4d_{5/2}$	247.8	Crushed	RU-1
	247.7	Crushed	F-6
	247.9	Crushed	B-2
	247.2	Crushed	D-1
	247.2	Crushed	GB-1
	247.5	Monolith	RU-1
	247.5	Monolith	F-2 and F-7
	247.5	Monolith	F-1
	247.4	Monolith	B-2
	247.2	Monolith	GB-1
W $4f_{7/2}$	35.9	Crushed	B-2
	35.5	Crushed	GB-1
	35.7	Monolith	B-2
Si 2p	104.4	Crushed	RU-1
	104.1	Crushed	F-6
	103.5	Crushed	B-2
	103.8	Monolith	RU-1
	103.7	Monolith	F-2 and F-7
	103.6	Monolith	F-1
	103.6	Monolith	B-2
	103.5	Monolith	GB-1
Al 2p	75.3	Crushed	F-6
	75.5	Monolith	F-1

the presence of a second Ti species (4 peaks in the Ti 2p doublet). Most likely, this feature is due to the algorithm used for background subtraction.

3.1.3. V 2p

The application of monochromated X-ray irradiation allowed a number of groups to avoid the problem connected with the proximity of V 2p doublet and the O 1s satellites. The remaining groups, which used non-monochromated radiation, tackled this problem either by satellite subtraction using standard software package (CH-2 and D-2) or by subtraction of the same range spectra measured after 10 min ion etching of the used monolith sample from the corresponding initial ones (RU-1). The 10 min etching results in practically complete disappearance of the V 2p lines from

Table 3
The mean values of core level binding energies determined from the data of Tables 2 and 3, as well as the deviation of the specific values from the corresponding mean ones (see text).

XPS region	Fresh sample		Used sample	
	E_b (eV)	Deviation	E_b (eV)	Deviation
Ti $2p_{3/2}$	459.0	0.0	459.0	0.0
C 1s	284.7	0.2	284.8	0.2
O 1s (1)	530.3	0.1	530.3	0.1
O 1s (2)	532.9	0.3	532.9	0.3
V $2p_{3/2}$	516.9	0.2	516.8	0.2
W $4d_{5/2}$	247.6	0.1	247.6	0.1
W $4f_{7/2}$	35.9	0.1	35.8	0.1
Si 2p	103.7	0.2	103.8	0.2
Al 2p	75.1	0.4	75.5	0.2

the spectra (see below). The mean values of V $2p_{3/2}$ binding energy of 516.9 eV for the fresh samples and 516.8 eV for the used ones (Table 3) allow us to assign this line to V(V) [6]. Contrary to the previous investigations of the V_2O_5/TiO_2 EUROOXIDE ELV1 catalysts [5] and the V_2O_5 standard sample (B-2), no asymmetry was detected in the V 2p spectra, testifying to the absence of V(IV) contribution. No reduction of V(V) was detected under vacuum and/or under X-ray irradiation (some of groups made two sequential acquisition runs). Moreover, even outgassing the samples at 300°C in vacuum for 30 min (RU-1, F-6) did not change the V 2p spectra. These results indicate that compared to V_2O_5/TiO_2 catalysts [5] the state of V(V) in the studied samples is much more stable. The increase in stability seems to be due to the presence of WO_3.

3.1.4. W $4f_{7/2}$ or W 4d

The assignment of the tungsten XPS lines is complicated by the large uncertainties in the determination of the W $4f_{7/2}$ binding energies due to overlapping with the other lines and the application of much broader tungsten line, W $4d_{5/2}$, which is not used usually to identify tungsten chemical state. However, deconvolution of the W 4f region carried out by some participants (F-2 and F-7, B-2) allowed us to determine the position of the main tungsten line: the mean value of the E_b(W $4f_{7/2}$) has appeared to be 35.7 eV, that is, characteristic of W(VI) [2,3]. Furthermore, by comparison to a reference [7] where the W $4d_{5/2}$ binding energies have been measured both for metallic W and for WO_3, the mean value of E_b(W $4d_{5/2}$) = 247.6 eV determined in this work (Tables 1 and 2) is much closer to the value characteristic of WO_3 (248.4 eV) than to that of the metal (244.2 eV) [7]. Considering the value of W $4f_{7/2}$ binding energy of 36.8 eV reported [7] instead of 35.9 eV measured in this work (Table 3), the coincidence of E_b(W $4d_{5/2}$) of our samples with that of the WO_3 becomes much better. No additional lines were observed for tungsten XPS spectra suggesting the existence of tungsten as W(VI) only.

3.1.5. C 1s

All participants assigned a component with the highest intensity in the C 1s spectrum to hydrocarbons chemisorbed on the catalyst surface. Indeed, the measured E_b value of 284.7 − 284.8 eV has been often used as a reference to take into account the charging effect [4]. Other C 1s lines deconvoluted by some participants from the total spectra were assigned to oxygen-containing groups of different chemical nature: 286.3 for *C*–O, 288.0 for O–*C*–O or *C*=O, 289.4 for O=*C*–OH [8].

3.1.6. Impurities

The Si 2p line with E_b = 103.7 eV (Table 3) can be identified as SiO_2, and Al 2p at about 75.1 eV as Al_2O_3. The higher value reported by some research groups (Tables 1 and 2) could arise from the differential charging of the impurity phases compared with the mixed oxide ones. Analysis of the S 2p (mainly as sulfate) as well as Pb $4f_{7/2}$ (Pb $4f_{7/2}$ at 139.8 eV, close to 140.0 eV in $PbSO_4$ [4]) lines detected on the monolith used sample allows one to conclude the formation of lead sulfate under working conditions.

In conclusion of this section, it should be noted that no conclusions about significant changes in the chemical states of the studied elements for the fresh and used samples can be made. The results show that the catalysts contain the mixed oxide elements in the highest oxidation state, V(V), W(VI) and Ti(IV), most probably as V_2O_5, WO_3 and TiO_2. To make an assumption about the surface model of these phases analysis of quantitative data is necessary.

3.2. Quantitative analysis

As compared to the binding energy values, much more significant discrepancies are observed in quantitative analysis. This affirmation is based on the results of the quantification expressed as atomic ratios of the observed elements to titanium shown in Tables 4 and 5. The quantification of the XPS spectra was carried out according to the first principle model using photoionization cross section, analyzer transmission and electron mean free path in a solid which are both kinetic energy dependent. Background subtraction was non-linear (Shirley type).

In addition, a number of participants have calculated the atomic fractions and, on this basis, the weight ratios of the oxides that have been used to be compared with chemical analytical data provided by Lercher from Twente University (Tables 6 and 7).

Table 4
The atomic ratios measured for the fresh catalyst

Fresh catalyst	Atomic ratio	Comments	Reference number
O/Ti	4.03	Crushed	RU-1
	3.18	Crushed	F-6
	4.36	Crushed	B-2
	4.96	Crushed	CH-2 and D-2
	4.55	Crushed	D-1
	4.5	Crushed	GB-1
	5.31	Monolith	RU-1
	6.81	Monolith	F-2 and F-7
	4.46	Monolith	F-1
	6.72	Monolith	B-2
	4.8	Monolith	GB-1
C/Ti	0.71	Crushed	RU-1
	0.87	Crushed	F-6
	1.66	Crushed	B-2
	0.71	Crushed	D-1
	1.2	Crushed	GB-1
	0.57	Monolith	RU-1
	0.63	Monolith	F-1
	1.60	Monolith	B-2
Si/Ti	0.28	Crushed	RU-1
	0.37	Crushed	F-6
	0.41	Crushed	CH-2 and D-2
	0.45	Crushed	GB-1
	0.49	Monolith	RU-1
	0.93	Monolith	F-2 and F-7
	0.78	Monolith	F-1
	0.75	Monolith	GB-1
V/Ti	0.11	Crushed	RU-1
	0.098	Crushed	F-6
	0.11	Crushed	B-2
	0.10	Crushed	CH-2 and D-2
	0.11	Crushed	D-1
	0.10	Monolith	RU-1
	0.073	Monolith	F-1
	0.12	Monolith	B-2
W/Ti	0.13	Crushed	RU-1
	0.068	Crushed	F-6
	0.098	Crushed	B-2
	0.081	Crushed	D-1
	0.19 (W 4f)	Crushed	GB-1
	0.12	Monolith	RU-1
	0.11	Monolith	F-1
	0.11	Monolith	B-2
	0.16 (W 4d)	Monolith	GB-1

Table 5
The atomic ratios measured for the used catalyst

Used catalyst	Atomic ratio	Comments	Reference number
O/Ti	4.10	Crushed	RU-1
	2.85	Crushed	F-6
	4.36	Crushed	B-2
	4.92	Crushed	CH-2 and D-2
	4.50	Crushed	D-1
	3.8	Crushed	GB-1
	7.42	Monolith	RU-1
	5.46	Monolith	F-2 and F-7
	4.62	Monolith	F-1
	6.42	Monolith	B-2
	5.1	Monolith	GB-1
C/Ti	0.54	Crushed	RU-1
	0.67	Crushed	F-6
	1.61	Crushed	B-2
	0.48	Crushed	D-1
	1.7	Crushed	GB-1
	1.58	Monolith	RU-1
	0.78	Monolith	F-1
	1.74	Monolith	B-2
Si/Ti	0.25	Crushed	RU-1
	0.31	Crushed	F-6
	0.38	Crushed	CH-2 and D-2
	0.33	Crushed	GB-1
	0.34	Monolith	RU-1
	0.64	Monolith	F-2 and F-7
	0.43	Monolith	F-1
	0.42	Monolith	GB-1
V/Ti	0.12	Crushed	RU-1
	0.097	Crushed	F-6
	0.11	Crushed	B-2
	0.10	Crushed	CH-2 and D-2
	0.17	Crushed	D-1
	0.052	Monolith	RU-1
	0.082	Monolith	F-1
	0.11	Monolith	B-2
W/Ti	0.14	Crushed	RU-1
	0.067	Crushed	F-6
	0.093	Crushed	B-2
	0.083	Crushed	D-1
	0.15	Crushed	GB-1
	0.14	Monolith	RU-1
	0.12	Monolith	F-1
	0.088	Monolith	B-2
	0.12	Monolith	GB-1

Despite the great variations in the results of different groups (Tables 4–7), one general trend is revealed by the results, namely enhanced weight contents of the introduced oxides (V_2O_5, WO_3, SiO_2, Al_2O_3) defined by XPS in comparison with the bulk level (Tables 6 and 7) demonstrating surface enrichment by these catalyst components.

The enrichment of the uppermost layers with V_2O_5, WO_3, SiO_2 and Al_2O_3 concluded from the data of Tables 6 and 7 indicates significant heterogeneity of

Table 6
The weight ratios of the oxides in the fresh catalyst

Fresh catalyst	Oxide weight ratio (wt.%)				
	Analytical data	XPS data			
		RU-1	F-6	RU-1	F-1
TiO_2	78%	55.5%	59%	51.4%	45%
V_2O_5	3.15%	6.9%	6.5%	5.9%	3.5%
WO_3	9%	20.9%	11.8%	17.8%	15.1%
SiO_2	6.5%	11.7%	16.6%	19.1%	30.6%
Al_2O_3	1.5%	5.0%	6.1%	5.9%	5.8%
Reference number	Lercher	RU-1 (powder)	F-6 (powder)	RU-1 (monolith)	F-1 (monolith)

the catalysts as a function of depth. Obviously, this together with the small XPS analysis depth (few dozens angstroms) highlights the limitation in using XPS (Tables 4–7) for quantitative analysis of the samples. Indeed, the TiO_2 phase can be masked by surface located particles of WO_3 and V_2O_5. Similar morphology has been shown previously for V_2O_5/TiO_2 catalysts [9]. To analyze this problem, the depth profiling of the catalysts by means of Ar or He bombardment has been carried out by one of the research groups (RU-1). Helium was used instead of argon in order to produce correct data on tungsten depth profiles: etching by argon would result in the accumulation of Ar into the subsurface catalyst layers and the detection of the Ar 2p doublet which overlaps the W $4d_{5/2}$ line. The results of these experiments can be seen in Figs. 3–5, where the dependencies of V/Ti, W/Ti and Si/Ti atomic ratios with time of ion etching are shown. One can see a sharp decrease in the atomic ratios with etching time for V and Si, whereas for tungsten the change in W/Ti atomic ratio is not so dramatic. The behavior of V/Ti and Si/Ti atomic ratios during ion bombardment supports the suggestion concerning surface location of these phases that can help explain the discrepancies of the quantitative data (Tables 4–7). The constancy of W/Ti atomic ratio can be explained by an intermediate location of the WO_3 phase between TiO_2 and V_2O_5 phases or a deeper penetration of tungsta within the bulk of the titania particles. The latter conclusion is confirmed by electrical conductivity measurement.

Detailed analysis of the dependencies presented in the Figs. 3–5 allows one to mark additional features in the depth concentration profiles:

1. The V/Ti atomic ratios for the used catalysts are lower than the corresponding ones for the fresh catalysts.
2. The initial Si/Ti atomic ratios (before etching) are higher for the monolith samples, but their decrease with bombardment time is much sharper than the corresponding profiles for the crushed samples.

Table 7
The weight ratios of the oxides in the used catalyst

Used catalyst	Oxide weight ratio (wt.%)				
	Analytical data	XPS data			
		RU-1	F-6	RU-1	F-1
TiO_2	78%	56.0%	61.4%	55.4%	47.4%
V_2O_5	3.15%	7.6%	6.8%	3.3%	2.5%
WO_3	9%	21.9%	11.9%	22.5%	14.6%
SiO_2	6.5%	10.5%	14.5%	14.2%	17.9%
Al_2O_3	1.5%	3.9%	5.4%	4.6%	–
Pb*	–	–	–	–	17.4%
Reference number	Lercher	RU-1 (powder)	F-6 (powder)	RU-1 (monolith)	F-1 (monolith)

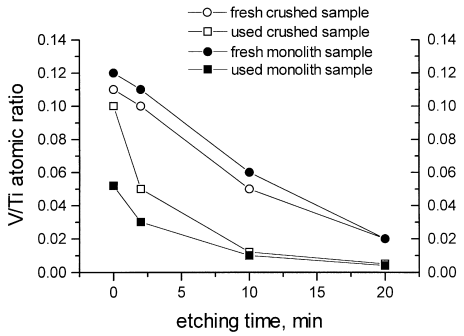

Fig. 3. The variation of V/Ti atomic ratios with time of ion etching.

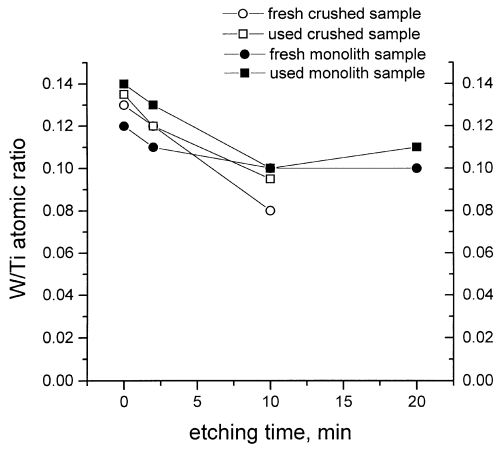

Fig. 4. The variation of W/Ti atomic ratios with time of ion etching.

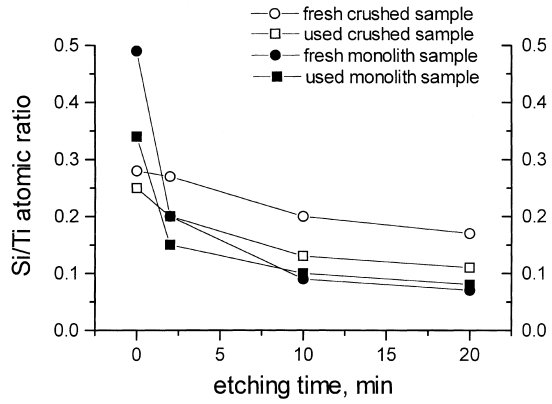

Fig. 5. The variation of Si/Ti atomic ratios with time of ion etching.

The former observation seems to be connected with the removal of the part of this phase from the XPS analysis depth during the operation of the catalysts in working conditions. There are two possible reasons for this phenomenon: dissolution of the vanadium into the bulk of TiO_2 or its escape into the gas phase. Unfortunately, XPS data cannot determine which of the factors is more significant. However, electrical measurements (see Chapter 8) indicate that V dissolves into TiO_2.

3.3. SIMS data

In full agreement with XPS results, positively charged ions both of the mixed oxide elements (Ti, TiO, Ti_2, Ti_2O, Ti_2O_2, Ti_2O_3, W, WO, V, VO) and of the impurities (C, CH, Si, Al, Ca, B and Pb on the monolith used catalyst) have been revealed in SIMS spectra. Mixed element signals such as WTi and WTiO ions were also measurable.

To analyze the depth distribution of the elements, the absolute intensities of fragment ion signals have been measured by mass spectrometer in sequence of sputtering scans (up to 80). Tables 8 and 9 present some selected fragment ion ratios for the fresh and used catalysts measured in first, 40th and last scans, i.e. on the sample depth. It should be noted that these data cannot be compared quantitatively with the XPS results (Tables 4 and 5), since they are presented as measured without any normalization. At the same time, the sensitivity factors for mass spectrometric measurements of V (21.5) and Ti (23.5) exceed the corresponding one for W (1.0) by more than 20 times [10]. This explains much lower values of W/Ti ratios in comparison with V/Ti ones although atomic ratios calculated on the basis of XPS are almost the same. In other words, the SIMS data presented in the Tables 8 and 9 should be considered comparatively: (i) for the fresh and used samples and (ii) on the depth of the samples.

One can see that for both the samples MeO/Me and CH/C ratios decrease sharply during argon sputtering. Such behavior of MeO/Me ratios can be explained by reduction of surface layers of V_2O_5, WO_3 and TiO_2 phases under argon impact. This suggestion is confirmed by XPS data, viz. shoulders on the low BE side of V $2p_{3/2}$, W 4d, Ti $2p_{3/2}$ spectra appear after the

Table 8
The selected fragment ion ratios measured by SIMS for the fresh catalyst (CH-2 and D-2)

Scan number[a]	V/Ti	W/Ti	TiO/Ti	VO/V	WO/W	WTi/Ti	CH/C
1	0.06	0.00026	0.098	0.079	0.47	1.22E-05	0.47
40	0.046	0.00022	0.057	0.03	0.28	1.57E-05	0.28
80	0.044	0.00024	0.041	0.021	0.28	1.54E-05	0.24

[a] See text.

first few minutes of Ar sputtering. The decrease in the CH/C ratios originates from removal of carbonaceous layers produced on the catalyst samples by hydrocarbon adsorption inside the spectrometer. The latter phenomenon depends on vacuum conditions, which can be different for different spectrometers, and, most probably, explains the great variation in C/Ti atomic ratios determined by XPS (Tables 4 and 5).

More complex dependencies of fragment ion ratios are observed for relative distribution of the mixed oxide elements. Indeed, if W/Ti ratios remain constant as the samples are etched by argon and are similar for the fresh and the used catalysts, so V/Ti ratios not only decrease with Ar sputtering, but also are characterized by much higher values for the fresh sample than those for the used one. These tendencies are in good agreement with XPS data and can be considered as additional corroboration for the suggestions concerning surface location of the V_2O_5 phase and its removal from the XPS analysis depth during the operation of the catalysts in working conditions. The consistency of the W/Ti ratios testifies a more homogeneous distribution of tungsta within the bulk of the titania particles in comparison with vanadia. This together with the slight increase in WTi/W ratios suggests that the WTi mixed element signals measured for the fresh sample originate from fragmentary ions existing in the original oxide matrix, but not form to a dominating extent during sputtering as result of association of the corresponding elements.

4. Conclusions

1. Both fresh/used and crushed/monolith samples exhibit similar binding energies of the XPS lines for all main elements (O, Ti, V, W) in the V_2O_5–WO_3/TiO_2 catalysts. This together with the stability of their XPS spectra under vacuum or/and under X-ray radiation allow us to identify the chemical states of these elements namely, Ti(IV), V(V) and W(VI). No other oxidation states for these elements were observed. The fact that the chemical shift results of all contributors are in reasonable agreement should be also emphasized.
2. Discrepancy in atomic ratios of the revealed elements can be proposed to arise from the heterogeneity of their composition as a function of depth. Ion etching data demonstrate that V_2O_5 phase, as well as other impurity ones, have a surface location with respect to TiO_2 and their redistribution occurs during catalyst operation, while tungsta is characterized by more homogeneous distribution within the bulk of the titania particles weakly changed under the influence of reaction conditions.
3. The other differences between samples are due to the presence of unexpected elements at the surface in significant percentages: Si (5–30%), Al (1–5%) in all samples and Pb and S in monolith used samples.

Table 9
The selected fragment ion ratios measured by SIMS for the used catalyst (CH-2 and D-2)

Scan number[a]	V/Ti	W/Ti	TiO/Ti	VO/V	WO/W	WTi/Ti	CH/C
1	0.028	0.00023	0.061	0.077	1.35	–	0.73
40	0.019	0.00025	0.008	0.015	0.27	–	0.29
80	0.018	0.00025	0.019	0.013	0.25	–	0.35

[a] See text.

References

[1] K. Siegbahn, C. Nordling, A. Fahlman, R. Nordberg, K. Hamrin, J. Hedman, G. Johansson, T. Bergmark, S.-E. Karlsson, I. Lindgren, B. Lindberg, ESCA. Atomic, Molecular and Solid State Structure Studied by Means of Electron Spectroscopy, Almquist and Winkler, Uppsala, 1967.
[2] M.P. Seah, Surf. Interface Anal. 14 (1989) 488.
[3] J.F. Moulder, W.F. Stickle, P.E. Sobol, K.D. Bomben, in: J. Chastain (Ed.), Handbook of X-ray Photoelectron Spectroscopy, Perkin Elmer, Eden Praine, 1992.
[4] D. Briggs, M.P. Seah, (Eds.), Practical Surface Analysis, 2nd Edition, Vol. 1, Auger and X-ray Photoelectron Spectroscopy, Wiley, New York, 1990.
[5] J.Ph. Nogier, M. Delamar, Catal. Today 20 (1994) 109.
[6] S.R.G. Carrazan, C. Peres, J.P. Bernard, M. Ruwet, P. Ruiz, B. Delmon, J. Catal. 158 (1996) 452.
[7] G.E. McGuire, D.K. Schweitzer, T.A. Carlson, Inorg. Chem. 12 (1973) 2450.
[8] P.A. Gerin, P.B. Dengis, P.G. Rouxhet, J. Chim. Phys. 92 (1995) 1043.
[9] M. DeBoer, Catal. Today 20 (1994) 97.
[10] G.R. Sparrow, Proceedings of the 25th Annual Conference on Mass-Spectrometry and Applied Topics, Washington, 1977.